

APPENDIX

for the paper

Pleistocene volcanism along the margins of the  
Canal de Ballenas transform fault, Gulf of California

by

**Arturo Martín-Barajas, Axel K. Schmitt, Bodo Weber,  
and Margarita López-Martínez**

*Published in Revista Mexicana de Ciencias Geológicas, v. 39, núm. 1, 2022, p. 16-26*

*DOI: <https://doi.org/10.22201/cgeo.20072902e.2022.1.1659>*

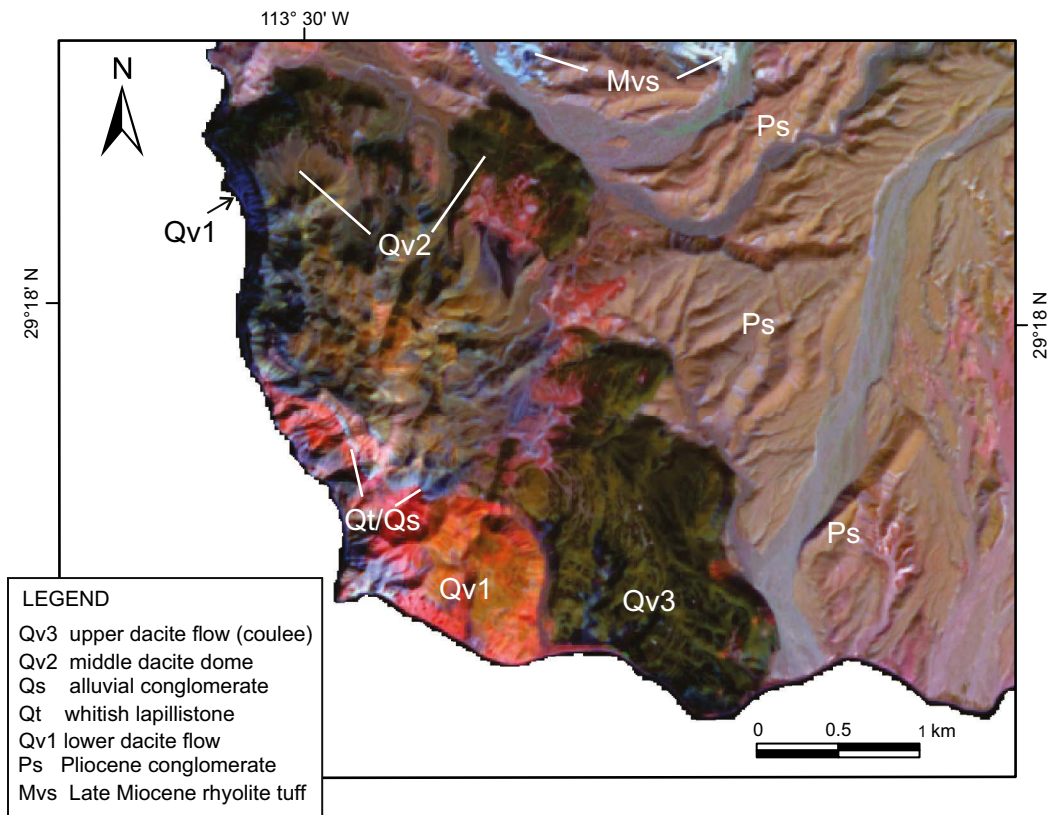


Figure S1. Spectral satellite image from EO-1 (30 m resolution) merged with the corresponding panchromatic image of 10 m resolution. Bands 7 (2.08-2.35  $\mu\text{m}$ ), 3 (0.63-0.69  $\mu\text{m}$ ) and 1 (0.45-0.515  $\mu\text{m}$ ) in Red, Green, and Blue channels respectively. Note contrasting color response of Qv3 and Qv1

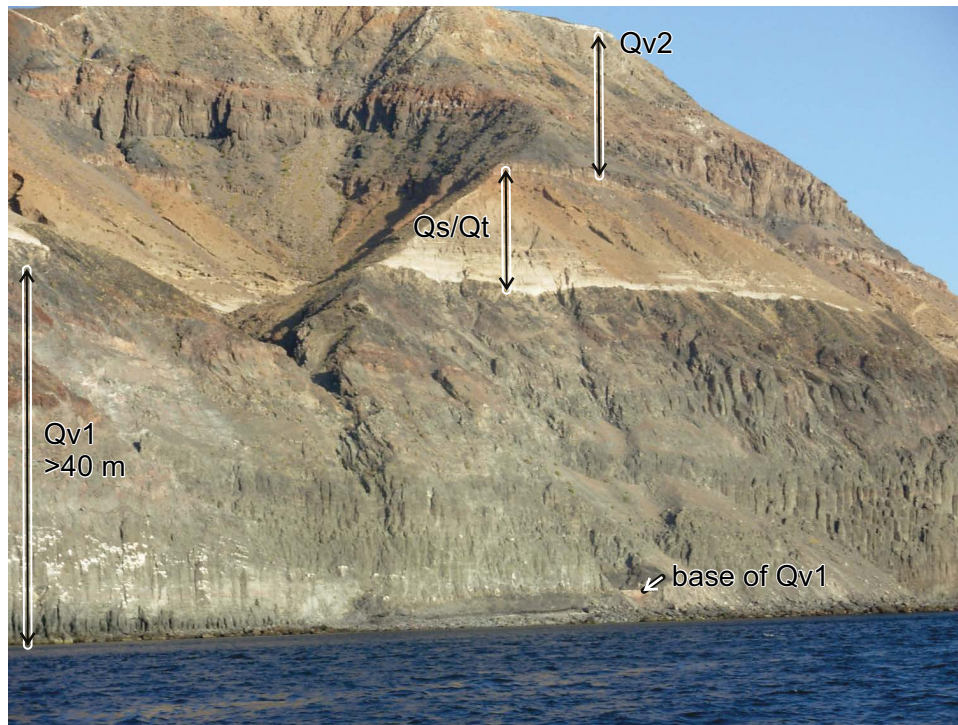


Figure S2. View west-southwest of the western cliffy shore of Lovera volcanic complex (LVC). The lower lava unit (Qv1) is >40m thick, displays columnar jointing and ramp structure. The overlying whitish unit (Qvt) is a pumice lapillistone, which is partially re-worked towards the top. Qvt grades upward into a well bedded sandy conglomerate (Qs) and underlies lava unit Qv2. The cliff is more that 200 m high. The summit of LVC reach 320 m above sea level.

Figures S3. Thin section photomicrographs of selected samples from Lobera Volcanic Complex (LVC) and Isla Coronado (ICO).

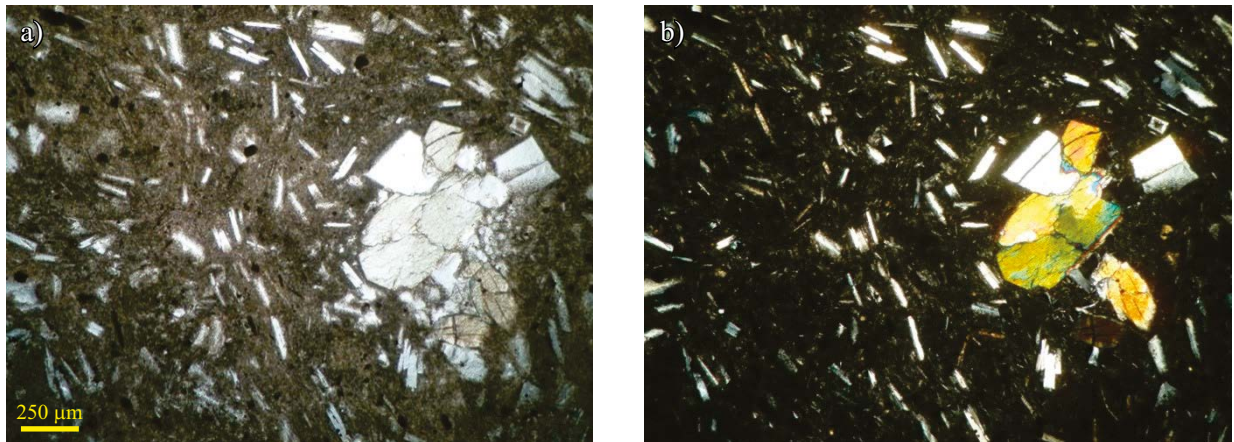


Figure S3-1. a) Thin section micrograph of sample IAG07-40, unit Qv2 of the LVC. Hypocrystalline texture of plagioclase microliths defining a flow texture (andesine-oligoclase) in a glassy matrix, with disseminated opaque minerals. Glomerophyric plagioclase (andesine) and clinopyroxene are common. b) Same image with polarized light, clinopyroxene shows yellowish and greenish interference colors.

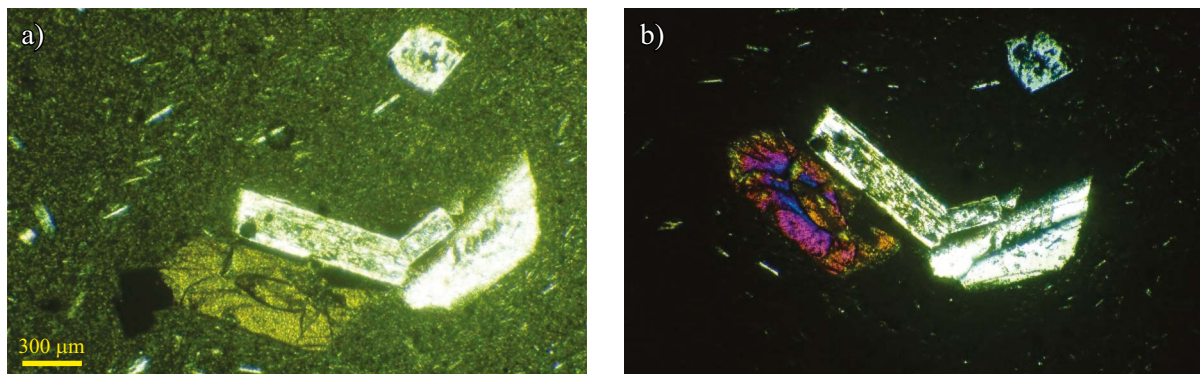


Figure S3-2. a) Micrograph of sample IAG07-38, unit Qv1 of the LVC. Hypocrystalline texture with fewer and smaller plagioclase microliths than in unit Qv2. Glomerophyric plagioclase, clinopyroxene and opaque minerals are common in the glassy matrix. b) Same micrograph with polarized light. Note the esquelital texture in plagioclase microphenocrysts.

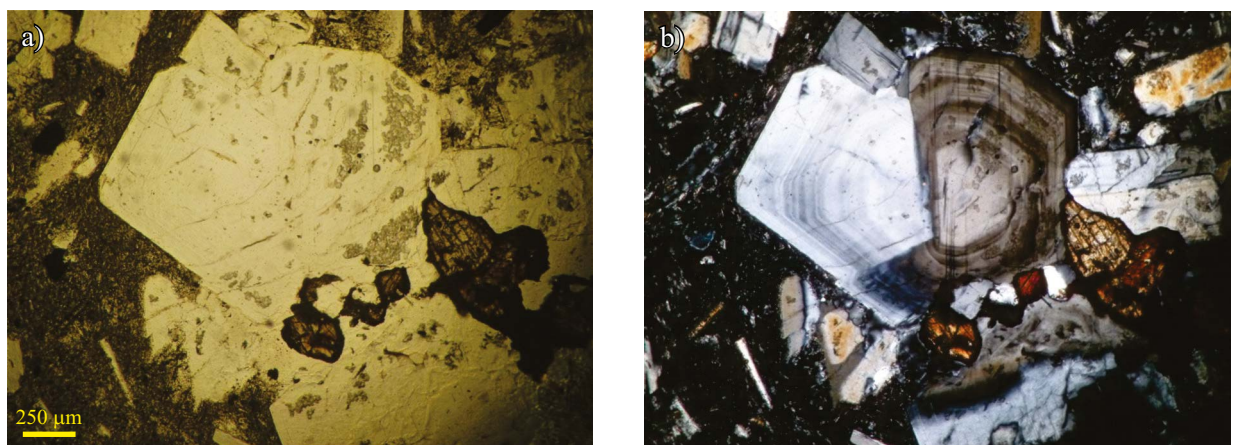


Figure S3-3. a) Micrograph of sample ICO08-1 with glomerophyric plagioclase, pyroxene and hornblende in a glassy matrix with plagioclase microliths. b) Same image with polarized light. Note the complex twinning and zoning of phyric plagioclase.

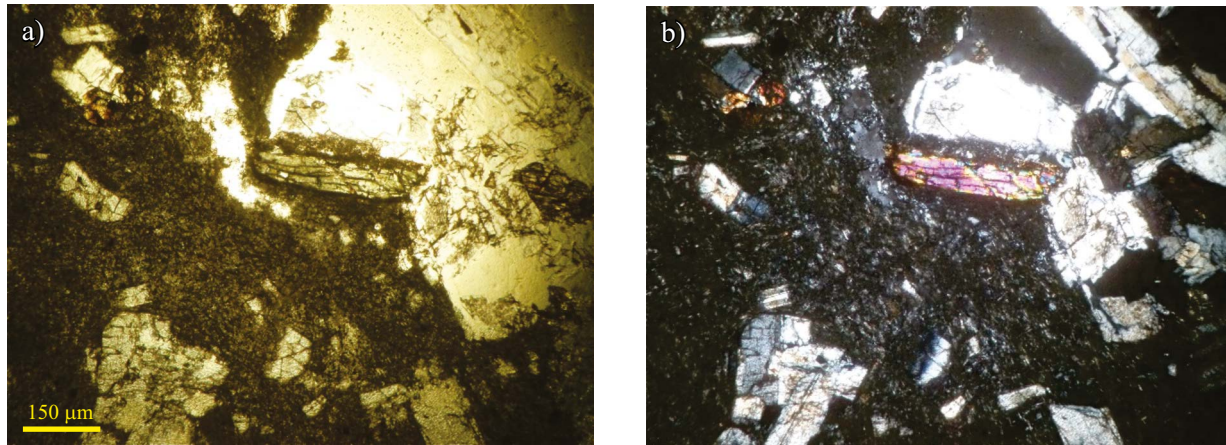


Figure S3-4. a) Micrograph of sample ICO08-3. Hypohyaline glomerophyric plagioclase and pyroxene are common in the partially devitrified glassy matrix, which also contains plagioclase microliths. b) Same micrograph with polarized light.

Table S1. Results of VG5400 laser step-heating experiments for whole-rock sample IAG07-40 corresponding to unit Qv2 of Lobera Volcanic Complex.

	Pwr	F <sup>39</sup> Ar	<sup>39</sup> Ar <sub>cum</sub>	Age	% <sup>40</sup> Ar <sub>atm</sub>	% <sup>40</sup> Ar*	<sup>37</sup> Ar <sub>Ca</sub> / <sup>39</sup> Ar <sub>K</sub>	
1 <sup>st</sup>	0.60	0.1549	0.1549	2474 ± 531	95.97	4.03	0.52	1
	1.10	0.2294	0.3843	350 ± 248	97.55	2.45	0.87	2†
	1.75	0.1562	0.5404	767 ± 218	94.85	5.15	1.19	3†
	2.60	0.1998	0.7402	778 ± 122	95.52	4.48	1.39	4†
	4.00	0.1782	0.9184	664 ± 184	97.14	2.86	1.42	5†
	7.00	0.0816	1.0000	394 ± 390	98.6	1.40	1.46	6†
2 <sup>nd</sup>	0.30	0.0307	0.0307	754 ± 1540	99.53	0.47	0.41	1
	0.80	0.2396	0.2703	1214 ± 263	95.35	4.65	0.64	2
	1.00	0.125	0.3954	264 ± 229	98.12	1.88	0.95	3
	1.60	0.1863	0.5817	459 ± 152	97.16	2.84	1.24	4
	2.50	0.1903	0.772	580 ± 189	96.99	3.01	1.50	5
	3.50	0.1123	0.8842	842 ± 236	96.37	3.63	1.49	6
	7.00	0.1158	1.0000	350 ± 306	98.75	1.25	1.47	7
Integrated results								
	<sup>39</sup> Ar	<sup>40</sup> Ar*/ <sup>39</sup> Ar <sub>K</sub>	Age	<sup>37</sup> Ar <sub>Ca</sub> / <sup>39</sup> Ar <sub>K</sub>	% <sup>40</sup> Ar <sub>atm</sub>	% <sup>40</sup> Ar*	<sup>40</sup> Ar/ <sup>36</sup> Ar	
1 <sup>st</sup>	6.70E-03	0.16 ± 0.02	889 ± 140	1.11	96.44	3.56	306.4	
2 <sup>nd</sup>	6.30E-03	0.12 ± 0.02	678 ± 133	1.14	97.34	2.66	303.6	

† Fractions used to calculate the plateau age given in the Figure 6.

#### <sup>40</sup>Ar/<sup>39</sup>Ar geochronology methods

The <sup>40</sup>Ar-<sup>39</sup>Ar ages were performed at Laboratorio de Geocronología of Centro de Investigación Científica y Educación Superior de Ensenada (CICESE). These were obtained in two laser step-heating experiments, the argon isotopic composition was measured with an VG5400 mass spectrometer. The sample preparation at Departamento de Geología at CICESE consisted of crushing and sieving, then rinsing with distilled water followed by 98 % acetone. The rock fragments were dried overnight at ~60 °C, and finally examined under the microscope to confirm that the sample is free of altered material.

The samples were irradiated with Cd liner in position 5C of the U-enriched research reactor of McMaster University in Hamilton, Ontario Canada. As irradiation monitors aliquots of sanidine TCR-2 (24.34 ± 0.28 Ma; Renne *et al.*, 1998) and sanidine FCT-2 (28.201 ± 0.046 Ma; Kuiper *et al.*, 2008) were used. The irradiation monitors were fused in one-step. Two laser step-heating experiments were performed with sample IAG07-40. All the argon extraction analyses were preceded by a blank measurement, where all the argon masses were measured. Upon blank subtraction, the argon isotopes were corrected for mass discrimination, calcium, potassium and chlorine neutron induced interference reactions. The parameters used to correct for neutron induced interference reactions were: (<sup>39</sup>Ar/<sup>37</sup>Ar)<sub>Ca</sub> = 6.50E-04; (<sup>36</sup>Ar/<sup>37</sup>Ar)<sub>Ca</sub> = 2.55E-04; (<sup>40</sup>Ar/<sup>39</sup>Ar)<sub>K</sub> = 0. Mass 36 was also corrected for chlorine derived <sup>36</sup>Ar (<sup>35</sup>Cl (n, γ) <sup>36</sup>Cl → <sup>36</sup>Ar + β with t<sub>1/2</sub> = 3.01×10<sup>5</sup> a). Isotopes <sup>37</sup>Ar and <sup>39</sup>Ar were corrected for radioactive decay. The constants recommended by Steiger and Jäger (1977) were used in all the calculations while all the straight line, calculations were performed with the equations presented in York *et al.* (2004). All errors are reported at 1σ level. The errors in the integrated, plateau and isochron age include the uncertainty in the J parameter. The integrated ages were calculated adding the fractions of the step-heating experiments (see Figure 6). The plateau age was calculated with the weighted mean of five consecutive fractions, which are in agreement within 1σ errors excluding the uncertainty in J. The data of the two experiments were plotted together in the <sup>36</sup>Ar/<sup>40</sup>Ar versus <sup>39</sup>Ar/<sup>40</sup>Ar correlation diagram to determine the isochron age and the initial <sup>40</sup>Ar/<sup>36</sup>Ar composition. The relevant <sup>40</sup>Ar-<sup>39</sup>Ar data are presented in the Supplementary Table S1.

#### REFERENCES

- Kuiper K.F., Deino A.L., Hilgen F.J., Krigman W., Renne P.R., Wijbran J.R., 2008, Synchronizing Rock Clock of Earth History: *Science*, 320, 500-504.
- Renne P.R., Swisher C.C., Deino A.L., Karner D.B., Owens T.L., DePaolo D.J., 1998, Intercalibration of standard absolute ages and uncertainties in <sup>40</sup>Ar/<sup>39</sup>Ar dating: *Chemical Geology*, 145, 117-152.
- Steiger, R.H., Jäger, E., 1977, Sub commission on Geochronology: Convention on the use of decay constants in Geo and Cosmochronology: *Earth and Planetary Science Letters*, 36, 359-362.
- York, D., Evensen, N.M., López Martínez, M., De Basabe Delgado, J., 2004, Unified equations for the slope, intercept, and standard errors of the best straight line: *American Journal of Physics*, 72 (3), 367-375.